SLAC – PUB – 4642
May 1988
(A)

BEAM PHASE SPACE DETERMINATION AT 50 GeV IN THE SLC LINAC*

JOHN T. SEEMAN
Stanford Linear Accelerator Center, Stanford University, Stanford, California 94309, USA
and
CHRIS ADOLPHSEN
University of California Santa Cruz, Santa Cruz, California 95064, USA

Abstract

The procedure for determining the six-dimensional phase space volume of high energy beams in the SLAC Linear Collider (SLC) requires multiple transverse profile and lattice measurements. The standard use of these measurements to determine the emittance and betatron functions is reviewed, and complications from anomalous dispersion are included. Anomalous dispersion influences betatron matching of the beams to downstream systems and affects the measurement of energy spectra. Techniques to measure the full beam sigma matrix and the corresponding TWISS parameters of beams with sub-100 μm sizes, one centimeter dispersions and 0.2% energy spectra are outlined.

Introduction

Electron and positron bunches at 1.15 GeV are injected into the SLC linac from the north and south damping rings and ring-to-linac transport lines, respectively. These beams are presently accelerated to 47 GeV separated into the two arcs and delivered to the final focus for collision [1]. The transverse beam phase space at the end of the linac is affected by size distortions of the beams entering the linac, alignment of the beams in the linac, the energy spectra along the linac, the quadrupole focusing lattice, transverse and longitudinal wake fields, and mismatched beams in the quadrupole lattice [2].

Measurements of the transverse phase space of the beams are obtained using intercepting and non-intercepting profile monitors. These measurements and the subsequent calculations are the subjects of this paper. The bunch length of the beam is determined by the ring-to-linac transport system and is measured using a streak camera and quartz radiator [3]. The energy spectra of the beams are measured using non-intercepting synchrotron radiation monitors in a dispersive region beyond the linac [4] and controlled using linac klystron phases.

Measurements of the beam size are frequently made to verify that the beam parameters have not changed due to linac or upstream changes. These measurements are used to calculate not only the phase space volume but also the orientation of the beam ellipse to compare with recent and design values. Three distinct types of data samples are obtained allowing different calculations to be performed.

1. One beam size measurement can estimate the emittance ϵ or the TWISS parameter β. $\sigma^2 = \epsilon\beta$.
2. Three beam size measurements using three lattice changes can determine ϵ, β and the TWISS parameter α.
3. Six beam size measurements using six lattice changes, three each in non-dispersive and dispersive optical regions, can determine ϵ, β, α, the energy spectrum δ, and the effective energy-position (angle) correlations d(d′) in the beam.

The first measurement requires a few minutes of beam time, the second 30–60 minutes, and the third two to three hours. The length of time depends on the number of steps in the procedure, compensation of quadrupoles that deflect the beams during adjustment, duplication of results, stability of the accelerator, and hardware problems such as radiation damaged regions on the fluorescent profile monitors.

Beam Conditions

Both electrons and positrons enter the linac from the ring-to-linac transport lines with horizontal and vertical emittances of 0.9×10^{-8} rad-m and 2.2×10^{-8} rad-m, respectively, at 1.15 GeV after extraction from the damping ring and bunch length compressed. The design emittance values are 1.3×10^{-8} rad-m. Typical values of the bunch length are 0.6 mm, the beam intensity 0.7×10^{10} particles, and the repetition rate 30 Hz. The energy spectrum is about 1%. The residual dispersion in the beam at the entrance to the linac is measured and corrected to be less than 1 cm in each plane. Both beams in the linac are accelerated on the same RF pulse and have their trajectories corrected simultaneously with dipole correctors located 12 m apart. The spacing is closer in the first 300 m. The typical residual trajectory has an rms value of 250 microns for both beams in both planes. An example is shown in Fig. 1. Slow feedback on the incoming and exiting beam launch parameters (x, x', y, y') of both beams occur once per minute. The electron energy is maintained at 47 GeV to within 50 MeV with a one minute per cycle feedback. The positron energy and the electron and positron energy spectra are maintained by the accelerator operators. These manual operations are performed every one to four hours.

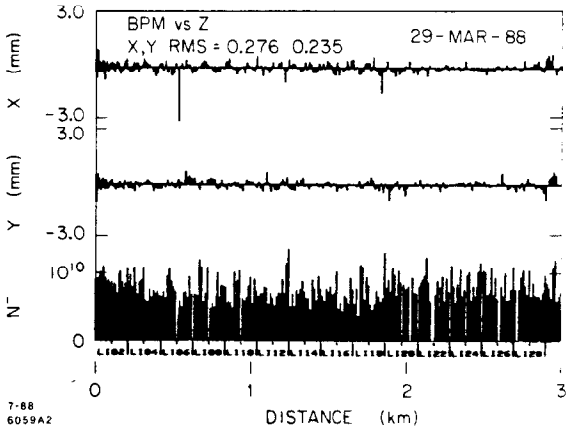

Fig. 1. Measured electron beam trajectory after computer trajectory correction of both electrons and positrons. The few large position offsets are due to broken electronic modules.

One Beam Size Measurement

A measurement of the transverse beam dimension is obtained by inserting a fluorescent profile monitor into the beam's path and viewing the size by a video television camera. A photograph of a single beam pulse is shown in Fig. 2. The video signal is digitized, the background is subtracted, and a

*Work supported by the Department of Energy, contracts DE–AC03–76SF00515 and DE–AA03–76SF00010.

numerical projection is computed. Figure 3 shows the horizontal projected profile of the image of Fig. 2. A gaussian fit to the projection gives a width σ of 128 microns for this example. This type of measurement is repeated many times per day and the width values are observed to vary slowly with extremes of about 50 to 250 microns.

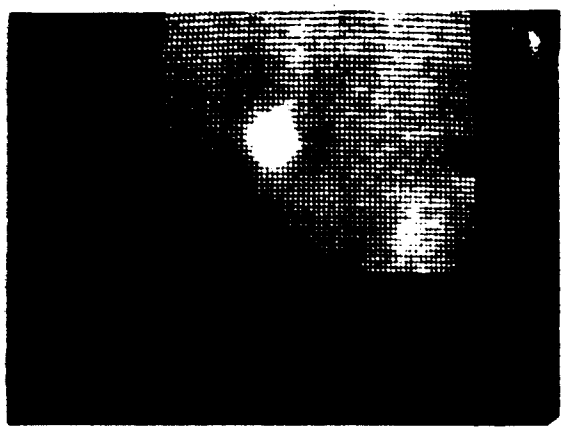

7-88 6059A3

Fig. 2. Electron beam transverse profile at 47 GeV on a profile monitor at the end of the linac. The central white spot is the beam image, the grid of white dots the digitization points, and the dark dots (4) the fiducial holes spaced apart 3 mm horizontally and 1 mm vertically.

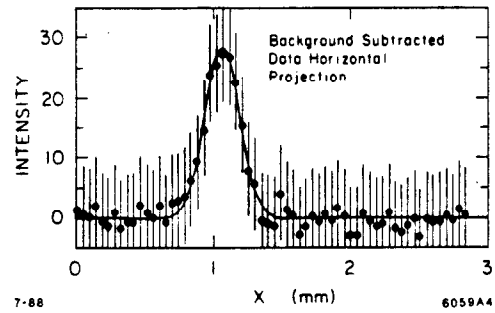

Fig. 3. Projected profile of the digitized beam image in Figure 2.

With one measurement a single beam parameter can be derived. The emittance is most often calculated

$$\epsilon = \frac{\sigma^2}{\beta} \qquad (1)$$

where β is the betatron function calculated from the present quadrupole lattice [2]. Horizontal x and vertical y measurements can be taken. The beam image of Fig. 2 gives a calculated emittance value of $\epsilon_x = 2.7 \times 10^{-10}$ rad-m assuming a β of 60 m. The design is 3.3×10^{-10} rad-m. This result is comforting except for the fact that the beam size varies by a factor of two throughout the day and thus, the apparent emittance by a factor of four. More detailed measurements and analysis shed light on this question. Finally, one can also calculate the effective β in the beam by assuming the emittance is known. $\beta = \sigma^2/\epsilon$.

Three Beam Size Measurements

Measurements of the beam size on a profile monitor as a function of the strength of an upstream quadrupole show a parabolic dependence of the beam size squared versus the quadrupole strength. From the three parameters of the parabolic fit, ϵ, β, and α can be calculated [5]. An alternate method of analysis is used here to emphasize how the TWISS parameters are transported, allows the addition of momentum dispersion of the beam into the calculation, and generalizes the problem so that multiple quadrupoles may be varied in the measurements.

The position x and angle x' of a particle can be transported from point A to point B using a transport matrix Rij, which is determined by the known optical elements between A and B [6]:

$$\begin{pmatrix} x \\ x' \end{pmatrix}_B \equiv \begin{pmatrix} R_{11} & R_{12} \\ R_{21} & R_{22} \end{pmatrix} \begin{pmatrix} x \\ x' \end{pmatrix}_A . \qquad (2)$$

The actual physical arrangement in the SLC is shown in Fig. 4 where quadrupole A is used to vary the beam size on profile monitor B. The β at position B can be calculated from the TWISS parameters β, α, and γ ($\beta\gamma = 1 + \alpha^2$) at location A using the known R matrix from A and B:

$$\beta_B = R_{11}^2\beta_A + R_{12}^2\gamma_A - 2R_{11}R_{12}\alpha_A . \qquad (3)$$

By multiplying Eq. 3 by ϵ, $\epsilon\beta_B$ can be identified as the beam size squared at position B:

$$\sigma_B^2 = \epsilon\beta_B = \epsilon R_{11}^2\beta_A + \epsilon R_{12}^2\gamma_A - 2\epsilon R_{11}R_{12}\alpha_A . \qquad (4)$$

If the quadrupoles between position A and B are varied so that three distinct R matrices, checked experimentally, and three corresponding beam size measurements are obtained, then three simultaneous equations like Eq. 4 are produced. Using Kramer's Rule, $\epsilon\beta_A$, $\epsilon\gamma_A$, and $\epsilon\alpha_A$ are extracted, and from $\beta\gamma = 1 + \alpha^2$, ϵ, β_A, α_A, and γ_A are calculated. Often, more than three measurements are taken for redundancy.

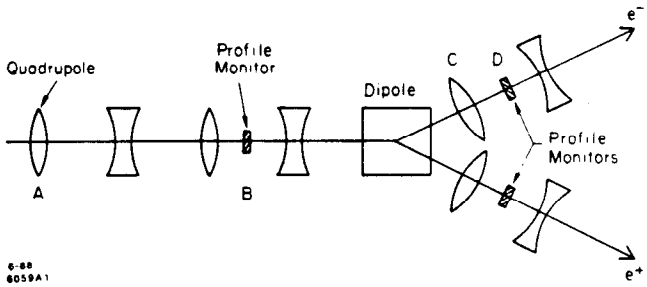

Fig. 4. Geometrical arrangement of the quadrupoles and dipoles at the end of the SLC linac.

An example is shown in Fig. 5 where the horizontal and vertical beam sizes were measured as a function of single quadrupole strengths. The data has been analyzed using Eq (4). The results are $\epsilon_x = 7.8 \times 10^{-10}$ rad-m, $\beta_x = 105$ m, $\alpha_x = 0.12$, $\epsilon_y = 7.7 \times 10^{-10}$ rad-m, $\beta_y = 37$ m, and $\alpha_y = -0.41$ given at a location immediately upstream of the measurement quadrupole. These values are good to about 30%. With this analysis method any or all of the quadrupole strengths between positions A and B could have been varied.

The emittance measurements here are about two times higher than the design values but tend to be fairly stable from day to day. The β and α calculated values vary more. Since the emittance exiting the linac is larger than that which entered, it

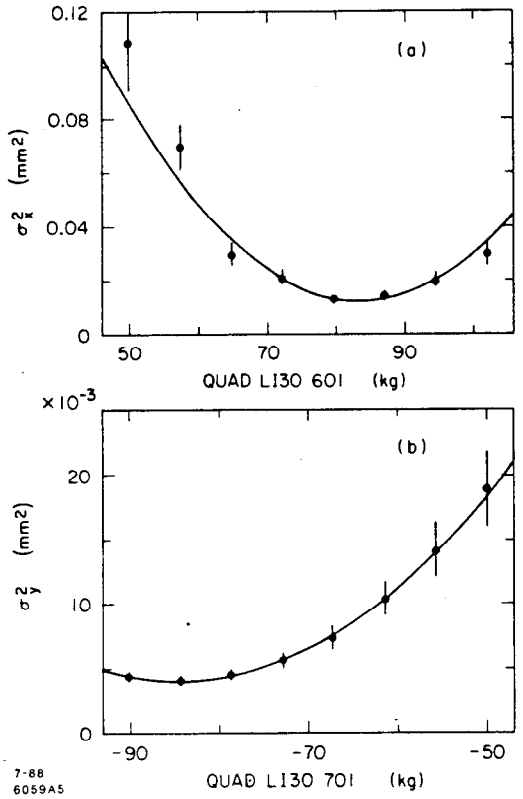

Fig. 5. Measured horizontal and vertical beam sizes versus quadrupole strength. There are three size measurements averaged per data point. Note that different quadrupoles are used for the two planes.

is believed to be caused by anomolous dispersion generated by steering the beam to off-axis quadrupoles and position monitors in the linac as is illustrated in Fig. 6. At the beam intensities of 0.7×10^{10} transverse wake field effects are not expected to contribute [2].

Effect of Momentum Dispersion on Emittance

If the beam has a momentum dispersion (transverse position-energy correlation) then the standard emittance measurement above will be corrupted. In order to include the effects, the position dispersion d, angular dispersion d' and the energy spectrum $\delta(=\sigma_E/E)$ must be included in the calculation. The beam size calculation becomes

$$\sigma^2 = \epsilon\beta + d^2\delta^2 \ . \tag{5}$$

The dispersion at position B can be calculated from the dispersion functions d and d' at A and the R matrix from A to B, assuming linear transport theory:

$$d_B = R_{11}d_A + R_{12}d'_A \ . \tag{6}$$

Inserting Eqs. 5 and 6 into Eq. 4 and following the above analysis procedure to determine ϵ, β, and α, an effective emittance as would be measured using the above method can be calculated showing how d, d', and δ contribute:

$$\epsilon^{eff} = \epsilon\left[1 + \frac{\delta^2[\beta_A d'^2_A + d^2_A\gamma_A + 2d_A d'_A\alpha_A]}{\epsilon}\right]^{\frac{1}{2}} \ . \tag{7}$$

Also, the effect on the calculation of β at position A is obtained:

$$\beta^{eff}_A = \frac{\epsilon\beta_A + \delta^2 d^2_A}{\epsilon^{eff}} \ . \tag{8}$$

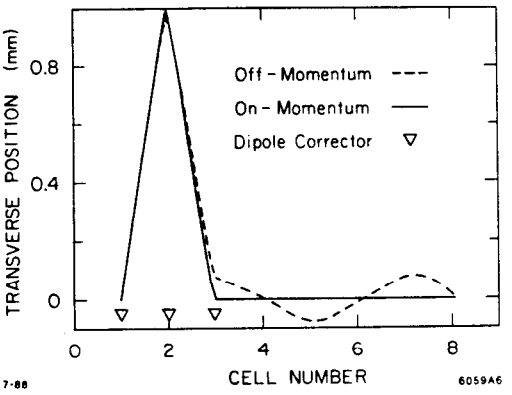

Fig. 6. Example of momentum dispersion generated by steering the beam through off axis quadrupoles. The off-momentum particle has a momentum error of 2%. The lattice has a phase advance of 90 degrees per cell. There are about 120 of these "bumps" in the SLC linac per plane with a random gaussian amplitude distribution of about 200 microns.

Thus, by the addition of dispersion, the actual ϵ and β are not determined correctly, which affects how the beam is handled and how the phase space is matched to the downstream systems. For example, if $\beta_A = 60$ m and $\epsilon = 3 \times 10^{-10}$ rad-m, then by the addition of $d = 4$ cm, $d' = 0$, and $\delta = 0.3\%$, $\epsilon^{eff} = \epsilon * 1.34$ and $\beta^{eff} = 81$ m. The effect gets worse as the energy spectrum increases.

Full Phase Space Measurements

All the unknowns in the beam in a given plane ϵ, β, α, δ, d, and d' can be determined by making three beam measurements each in non-dispersive and in dispersive beam transport regions. In the SLC the configuration is shown in Fig. 4. Beam size versus quadrupole setting data are taken with quadrupole–profile monitor pairs A-B and C-D. The region C-D has a non-zero dispersive R matrix as generated by the beam separating dipole. The A-B region has zero dispersion in the R matrix. The dispersion d near the quadrupole C and profile monitor D is about 7 cm. The beam energy and energy spectrum are traditionally measured here. The analysis below uses all the simultaneous measurements to determine the beam quantities at position A. Quadrupole C is part of a dipole alternating gradient magnet which makes it difficult to vary more than about 10% in strength. The profile monitor D is a non-intercepting synchrotron radiation monitor [4]. These measurements cannot be made at present in the vertical plane as there is no vertical bending to produce vertical dispersion.

The data analysis uses the SIGMA matrix of TRANSPORT [6] to calculate the beam size at the appropriate measurement point as computed from the known R matrices and initial beam conditions. Due to the number of elements in the transport line the equations are quite large but can be represented in a simple form:

$$\begin{aligned}\sigma^2_B = {} & f(A,C)[\epsilon\beta_A + d^2_A\delta^2] \\ & + g(A,C)[-\alpha_A\epsilon + d_A d'_A\delta^2] \\ & + h(A,C)[\epsilon\gamma_A + d'^2_A\delta^2] \\ & + S(A,C)[d_A\delta^2] \\ & + t(A,C)[d'_A\delta^2] \\ & + u(A,C)[\delta^2]\end{aligned} \tag{9}$$

where f, g, h, s, t, and u are long but simple expressions of R matrix elements between positions A and B or A and D. Once

the quadrupole values of A and C are determined, f through u are uniquely given. The expressions in the square brackets are just the elements of the SIGMA matrix expressed in terms of ϵ, β, α, d, d', and δ. The matrix elements associated with functions f through u are σ_{11}, σ_{12}, σ_{22}, σ_{16}, σ_{26}, and σ_{66}, respectively.

The careful, but not difficult, choice of three independent quadrupole settings for A and C leads to six independent sets of functions, f, g, h, s, t, and u and thus, six independent beam size measurements. Again, Kramer's Rule can be used to determine the six quantities in square brackets in Eq. 9. Those six quantities can be subsequently analyzed to reveal ϵ, β_A, α_A, δ, d_A, and d'_A.

This technique has become available only recently and has been used only a few times due to the difficulty in taking the measurements. The results of a data set taken in March 1988 are shown in Table 1. The results indicate that the beam has the correct emittance but that it has a large dispersion component and a large betatron mismatch. It is not known whether these results are stable day-to-day. However, this technique shows promise to reveal the full parameters of the beams.

Table 1. Full beam parameter calculation at 47 GeV.

Parameter	Three Measurements	Six Measurements	Design
$\epsilon_x(r-m)$	7.8×10^{-10}	3.1×10^{-10}	3×10^{-10}
$\beta_x(m)$	105	131	60
α_x	0.12	−0.47	-3
$d_x(m)$	0	−0.056	0
d'_x	0	0.0002	0
δ (%)	—	0.34	0.2

In the future this technique will be improved by reducing the measurement errors as many additions and subtractions have to be made in the analysis, by reducing the time required for data collection, by improving hardware (quadrupole C), and by finding a method to make measurements in the vertical plane.

Acknowledgments

Many people at SLAC have contributed to emittance measurement techniques on the SLC. We wish to thank them for their help in producing the beams, instruments, software, and analysis methods. Special thanks are extended to W. Atwood, J. Sheppard, P. Morton, M. Ross, R. Servranckx, and H. Shoaee.

References

[1] J. Seeman and J. Sheppard, *Status of the SLC*, Workshop on New Developments in Particle Accelerator Techniques, p. 122, 1987; also SLAC-PUB-4421.

[2] J. Seeman and J. Sheppard, *Special SLC Linac Developments*, Stanford Linear Accelerator Conference, p. 214, 1986.

[3] J. Sheppard et al., *Real Time Bunch Length Measurements in the SLC Linac*, IEEE NS-32, No. 5, Particle Accelerator Conference, p. 2006, 1985.

[4] J. Seeman et al., *SLC Energy Spectrum Monitor Using Synchrotron Radiation*, Stanford Linear Accelerator Conference, p. 441, 1986.

[5] M. Ross et al., *High Resolution Beam Profile Monitors in the SLC*, IEEE NS-32, No. 5, Particle Acclerator Conference, Vancouver, p. 2003, 1985.

[6] K. Brown, *A First- and Second-Order Matrix Theory for the Design of Beam Transport Systems and Charged Particle Spectrometers*, SLAC Report-75, June 1982.